Total detachment cross sections of C^-, CH^-, C_2^-, and C_2H^- incident on N_2 at keV energies

R. F. Nascimento,[1] S. L. A. Mello,[2] B. F. Magnani,[2] M. M. Sant'Anna,[2] Ginette Jalbert,[2] and N. V. de Castro Faria[2]
[1]*Centro Federal de Educação Tecnológica Celso Suckow da Fonseca, Campus Petrópolis, 25620-003, Petrópolis, Brazil*
[2]*Instituto de Física, Universidade Federal do Rio de Janeiro, Caixa Postal 68528, Rio de Janeiro, 21941-972, RJ, Brazil*
(Received 8 March 2013; published 10 June 2013)

We have measured the total electron detachment cross sections of the negative ions C^-, CH^-, C_2^-, and C_2H^- incident on molecular nitrogen in the velocity range 0.22–0.56 a.u. The data were measured with reliable normalization and, particularly in the critical case of the C^- projectile, the absence of beam contamination due to long-lived metastable states. Comparison of all measurements of cross sections with experimental data for other projectiles shows a common velocity dependence with a maximum near 0.4 a.u. This behavior suggests a connection between the anion-N_2 electron-loss collision dynamics and that of the shape-resonance process dominant in low-velocity electron-N_2 total electron scattering.

DOI: 10.1103/PhysRevA.87.062704 PACS number(s): 34.50.Fa

I. INTRODUCTION

Neutral and charged carbon clusters, C_n, and carbon monohydrides, C_nH, have been the subject of several experimental [1–4] and theoretical studies [5–7]. In particular, the study of their corresponding negative ions (anions) represents a key step in understanding astrophysical environments [8–10] and the chemistry of the interstellar medium (ISM) [11]. In fact, many of the anion species detected in space are carbon based, and among the first detected species are C_nH^- ($n = 4,6,8$) [12–14] and C_nN^- ($n = 3,5,7$) [15–17]. The formation mechanism of the former is often identified with direct electron attachment to their neutral counterparts [18], while the latter is produced in reactions involving carbon clusters C_n and N atoms. In addition to being found in the ISM, C_nH^--type anions have also been detected in a few different scenarios within our solar system [8, 19]. These anions also have a prominent role in the unwanted formation of dust in tokamak devices. In this latter case, when trapped, the small anions may work as a seed for the nucleation of microscopic particles composed of C and H [20,21].

From planetary moons' atmospheres to the coma of Halley's comet, small mass groups (7–65 amu) of anions have been detected and identified with C^-, CH^-, C_2H^-, and CN^-. In the latter case, they are formed via sputtering of cometary ice induced by solar radiation. Despite the growing interest which followed recent discoveries, very little is known about the interaction of these anions (e.g., reaction rates, stability, etc.) with other components that constitute such astrophysical media [22]. In order to have a better picture of the problem, further experimental investigation making use of ion traps or ion storage devices [23–27] is needed to mimic conditions found in the media of astrophysical interest. As an important parameter regarding the stability conditions of an ion trap, the number of ions within the trap must be suitably controlled. Moreover, it is known that the number of anions in such traps decays with time due to electron loss processes occurring in collisions between the anions and the residual gas. The beam lifetime is inversely proportional to the anion destruction cross section [28]. In experiments involving crossed or merged beams the role of residual gas is usually critical, even when ultrahigh-vacuum conditions are optimized (e.g., [29]).

In this paper we present total electron detachment (TED) cross sections (also called total electron loss cross sections) for C_n^- and C_nH^- ($n = 1,2$) projectiles incident on molecular nitrogen. Projectiles in the keV range spanned the velocity range from 0.22 to 0.56 a.u. For the C^- projectile the data available in the literature display normalization differences by factors up to 20. Beam contamination by long-lived metastable C^- ions may be partially responsible for theses discrepancies. Measuring mass spectra from the ion source, we analyze and exclude the potentially inconvenient effect of the long-lived metastable contribution for our C^- ion beam. To our knowledge, the CH^- and C_2H^- TED cross sections due to anion impact on N_2 (the main constituent of our atmosphere and common residual gas in vacuum beam lines) cannot be found in the literature.

Comparison with experimental data for other anionic projectiles suggests a universal behavior of cross sections related to that of the total electron scattering by N_2, dominated in this velocity range by a shape resonance. This universality highlights the reliability of the normalization procedure utilized. It also suggests key elements to be taken into account in future theoretical calculations for collision systems involving CH^- and C_2H^- projectiles.

II. EXPERIMENTAL METHOD

A. Production and selection of negative-ion beams

The negative ions are produced by a sputtering ion source from the National Electrostatics Corporation (NEC) developed originally by Middleton and Adams [30]. We use as a sputtering target high-purity graphite in powder mixed with hydrogen peroxide (H_2O_2). The sputtering of cesium on this sample produces negatively charged carbon clusters and compounds containing hydrogen and oxygen which are extracted and mass separated. This setup yields up to milliampere beam currents in the case of C^- and a relative C_nH^- beam intensity of about 30–60% of the C_n^- current. The amount of CH^- and C_2H^- emerging from the cathode diminishes with time. Typically, it decreases by a factor of 2, smoothly, after several hours. Each cross-section measurement takes around a few minutes. Thus, the intensity of the incident beam is approximately constant during each cross-section measurement.

 ©2013 American Physical Society

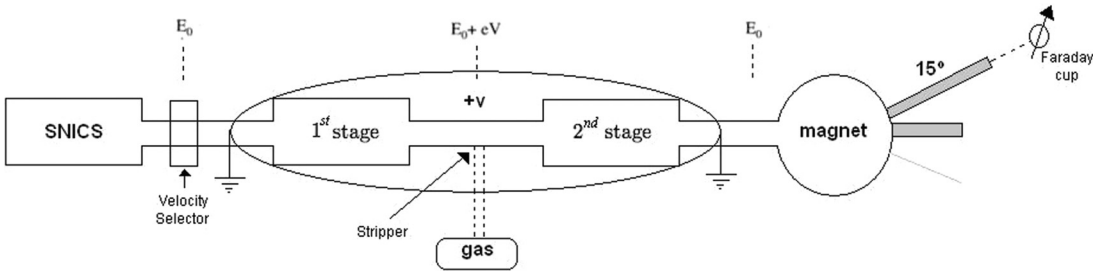

FIG. 1. Schematics of our accelerator.

B. Measurement of total detachment cross section

To measure total detachment cross sections of collisions involving negative ions, we employ a method that uses the center of a tandem accelerator as the target gas cell itself. Details about the method and our experimental setup were given in previous publications [31–37], and only the main features are described here. The method is based on the use of the high-voltage terminal as the collision chamber, with the collision target being what is traditionally used only as a gas stripper to produce positive ions and neutral species at the second stage of the accelerator. Without any physical change in the accelerator, we use it in a different mode.

Molecular nitrogen gas is admitted in the central part of the accelerator from an outside bottle, as usual. Total detachment cross sections for these collisions may be obtained provided the target pressure is known. Basically, a negative ion beam is extracted from a sputtering ion source, gets an energy E_0 of a few keV, is mass analyzed by a Wien filter, and enters the first accelerating stage of the tandem (Fig. 1). At the tandem high-voltage terminal, these ions collide with the atoms or molecules of the stripper gas. The collision energy is $E_0 + eV$, where V is the tandem high voltage. The target gas species and pressure can be very easily controlled from outside the vessel. The negative ions that survive traversing the gas target are decelerated back to their initial energy E_0, allowing their charge-state selection to be made with a small magnet, even for heavy ions. Subsequently, the charged fragments are separated by a magnetic analyzer and detected with Faraday cups. An attenuation curve of the negative ion beam emerging from the gas cell is then measured as a function of the target pressure.

In this velocity range, negative ions present a negligible reconstitution probability (by electron capture in a second collision) after being destroyed. The measured current I that traverses the gas is given by

$$I = I_0 k_1 k_2 e^{-\sigma\pi} = I_0' k_2 e^{-\sigma\pi}, \tag{1}$$

where σ is the total electron detachment cross section, k_1 and k_2 are the respective transmission probabilities for the negative ion in the first and the second tandem stages, I_0 and I_0' are the respective negative ion currents entering the tandem and reaching the gas target stripper, and π, given by the product of the target length L and its density, is the target thickness in particles per unit area.

$$\pi = P_{st} L / k_B T, \tag{2}$$

where k_B is the Boltzmann constant, T is the absolute temperature, P_{st} is the stripper pressure, and L is the target length. Both k_1 and k_2 transmission probabilities may be substantially smaller than unity due to space charge and beam defocalization effects. Nevertheless, as they depend only on the terminal voltage and not on the target pressure, the measured current I still presents an exponential dependence on the $\sigma\pi$ product, and the attenuation method may then be employed as usual to obtain the destruction cross-section values.

An external container feeds the stripper chamber with the nitrogen gas, whose purity is of 99.99%. The gas pressure is regulated by the opening or closing of an internal admission valve. As the stripper is kept at a high potential, no pressure gauge is available there, and the stripper pressure is not directly known. In order to access the true stripper pressure, a preliminary calibration procedure is performed. A beam of 1-MeV hydrogen negative ions traverses the stripper gas target, and the resulting neutral beam current is measured as a function of the pressure readings on the high-energy end (beam exit) pressure gauge. Published experimental values of the hydrogen beam charge changing cross sections and the rate equations for the charge state populations are then used to calculate the expected neutral fraction F_0 as a function of the true stripper pressure. We have chosen for pressure calibration the reliable cross-section values from the review of Nakai *et al.* [38] for H^-, H^0, and H^+ beams. By scaling our experimental values for the charge changing of H^0 on N_2 to the calibration values, we obtain the relation between the high-energy end pressure and the true stripper pressure [31]. In Fig. 2, the results of both the measured and the calculated neutral beam fractions F_0 are shown. The factor used to scale the experimental results to the theoretical ones is used to obtain the true stripper pressure from the high-energy end pressure. This factor is beam independent and can be used for all anionic projectiles incident on N_2

The uncertainties in the high-energy pressure are lower than 1%, leading to a target pressure uncertainty of about 7%, mainly coming from the uncertainties in the published cross sections introduced in the analytical expressions. The fitting procedure for attenuation curves introduces an error of about 10%. The global error, combined in quadrature, is of the order of 12%.

III. RESULTS AND DISCUSSION

With the method briefly discussed earlier, we produce several anionic carbon species with different mass-to-charge ratios. We then measure the attenuation of C_n^- and C_nH^- ($n = 1,2$) on N_2 and, by fitting an exponential decay curve, extract their cross sections.

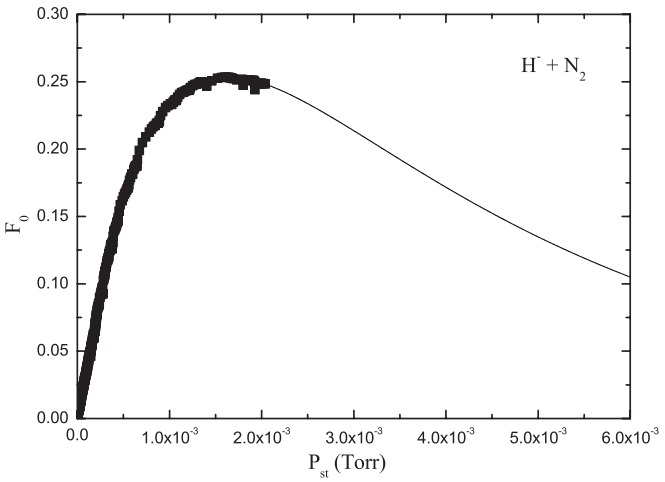

FIG. 2. Neutral fraction F_0 as a function of the true stripper pressure for charge changing of H^- in collisions with N_2. Line, theoretical results calculated with the rate equations for charge-state populations; squares, our experiment results normalized to the theoretical results.

A. Mass-to-charge spectra

In the Figs. 3 and 4, we show some of the products derived from our sputtering source. We note that the sputtering of a H_2O_2-mixed carbon-rich sample represents a viable source for the production of C_n^- and C_nH^- ($n = 1,2$). The anions of interest are then separated on a magnet so that their corresponding current attenuation can be measured on the Faraday cup displayed in Fig. 1.

It is important to note that the assumed CH peak (13 amu) shows a total relative intensity of approximately 30% in relation to the carbon peak (12 amu) intensity. This relative intensity vastly exceeds the known abundance of the ^{13}C isotope, which is about 1%. For the C_2H^- beam, the relative intensity can reach up to 50% of the C_2^- peak. Therefore, the ^{13}C isotope contamination on the C_nH^- ($n = 1,2$) beam is considered negligible throughout this work.

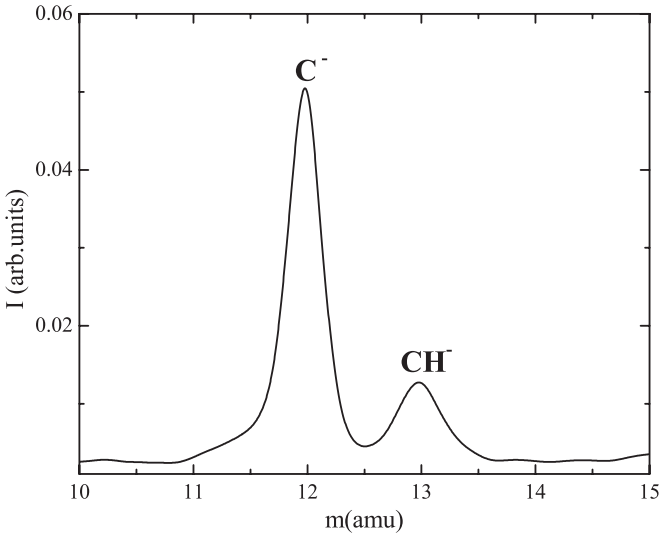

FIG. 3. Mass spectrum at the region of the C^- and CH^- peaks obtained from the sputtering of the H_2O_2-mixed graphite sample. Note that the relative intensity between mass 13 (CH^-) and mass 12 (C^-) peaks greatly exceeds what would be expected from the natural isotopical abundance of carbon (see text).

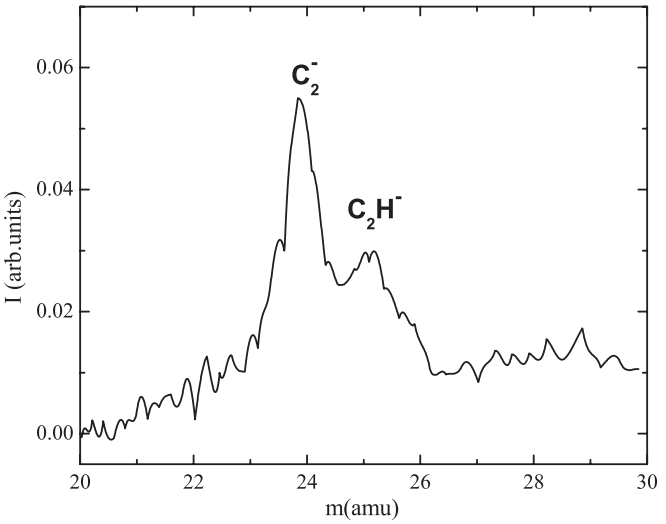

FIG. 4. Same as Fig. 3, but for the C_2^- and C_2H^- peaks.

B. Total electron detachment cross sections

After preparing and selecting the anions of interest, we proceed to measure their current attenuation on the Faraday cup. For the purposes of this work, we assume that the probability of electron capture at a subsequent collision after the anion destruction is negligible. A typical current attenuation curve is shown in Fig. 5. We note that the beam current decays exponentially until the stripper pressure reaches a limit of $P_{st} \sim 10^{-1}$ Torr. The one-exponential fitting curve indicates that either the fraction of metastable C^- anions in the beam is negligible or that the cross sections for ground-state and metastable C^- projectiles are very similar; otherwise

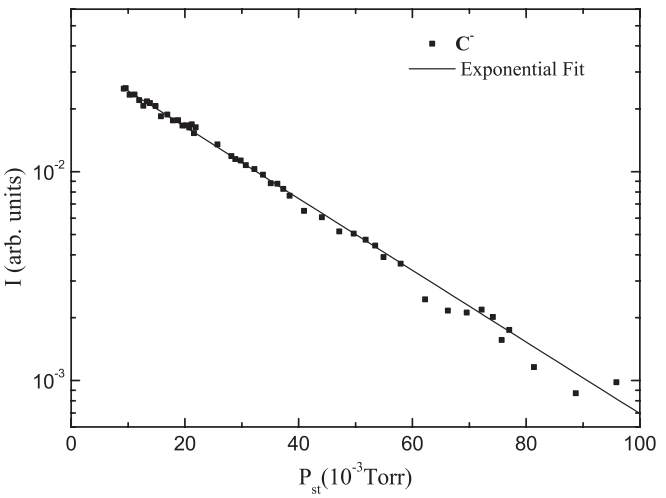

FIG. 5. Current attenuation curve for C^- on N_2 for $v = 0.34$ a.u. and a one-exponential fitting curve. The fitting indicates that either the fraction of metastable C^- anions in the beam is negligible or that the cross sections for ground-state and metastable C^- projectiles are very similar (see text).

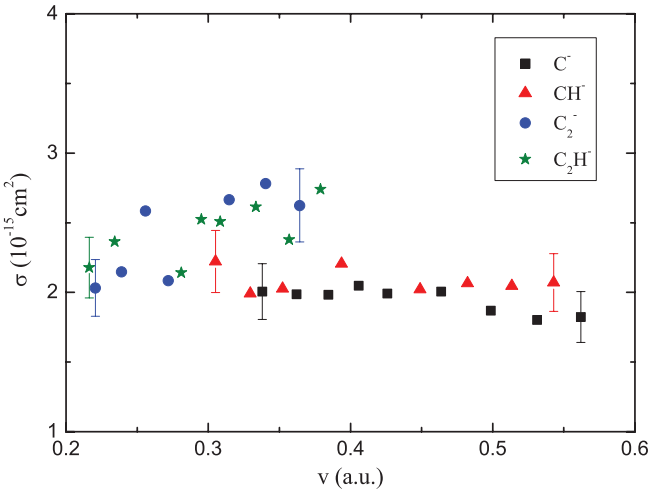

FIG. 6. (Color online) Electron detachment cross sections as function of the impact velocity. Black squares, C^-; red triangles, CH^-; blue circles, C_2^-; green stars, C_2H^-.

a two-exponential curve would be present [39]. Therefore, we may neglect the influence of the metastable C^- anions in our TED cross-section measurements. The uncertainties associated with the fitting process are no greater than 10%.

The TED cross sections for C_n^- and C_nH^- ($n = 1,2$) are shown in Fig. 6. We note that although the cross sections vary with the anion order ($n = 1,2$), the difference between the TED cross sections of plain carbon anions and their hydrogenated counterparts is very small.

To our knowledge, TED cross sections of C_nH^- colliding on N_2 are not available in the literature. However, other groups have studied collisional destruction of C^- on many target systems, including N_2. In Fig. 7, we compare the present results for collisional destruction of C^- with results published by four other groups [40–43]. As can be noted from Fig. 7, there are major discrepancies between the results obtained from different groups. These discrepancies reach up to a factor of 20, which may indicate normalization problems in the different experimental procedures used. The presence of unidentified fractions of metastable C^- ions in the beams used in the determination of C^- cross sections is another possible cause for the large discrepancies among data from different experimental groups (see Fig. 7).

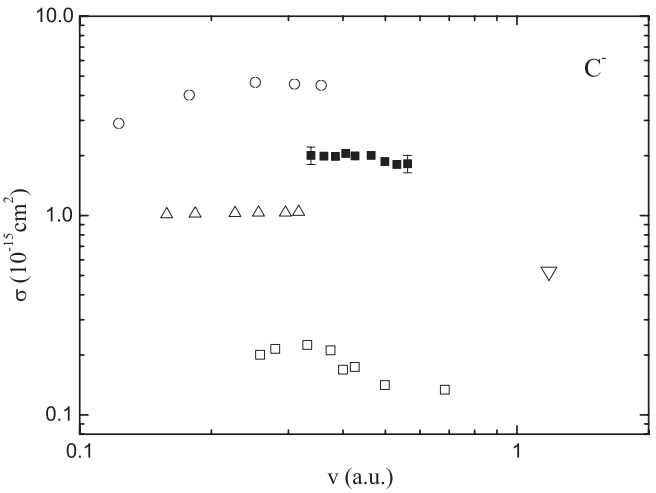

FIG. 7. Comparison of the TED cross sections for C^- on N_2 as a function of the impact velocity measured by different groups. Open circles, Ref. [40]; solid squares, present results; upward triangles, [41]; inverted triangles, [42]; open squares, [43].

As opposed to being directly produced from an anion sputtering source as in the present study, the C^- beams used in Refs. [41–43] were produced via double electron capture of C^+ in collisions with gaseous targets. In such processes the C^- ion is predominantly produced in its metastable ^2D and ^2P excited states (see Ref. [44], and references therein). Moreover, in the aforementioned experiments, the anion destruction cross sections were determined via direct detection of the neutral carbon atoms after the anions traversed the collision chamber. In doing so, the destruction cross sections become highly susceptible to the detector efficiency, which is not discussed in detail in those papers. The problem of detecting neutrals with accurate efficiency determination is avoided in the present paper since we measure the attenuation curves (exponential decays) of the C^- beam current.

It must be noted that in Ref. [40], the anion source is similar to the one used in the present paper (sputtering ion source), and therefore we discard the possibility of any considerable fraction of metastable ions in that work (see Fig. 7). However, neither the normalization procedure nor the kind of pressure gauge is discussed in the paper. In particular, the pressure conditions within the gas cell must be suitably controlled.

Figure 8 shows our results for C_n^- ($n = 1,2$) with TED cross sections of other anions impacting on N_2 measured by different groups. It is known that the TED cross sections follow the trend of electron-scattering cross sections for several target systems [45]. For electron scattering on N_2, shape resonances

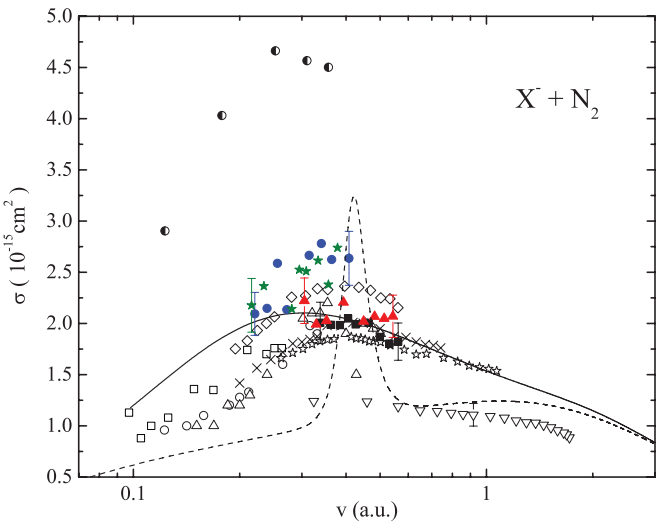

FIG. 8. (Color online) TED cross section of various anion projectiles impacting on N_2. Solid black squares, our results for C^-; solid blue circles, our results for C_2^-; solid red triangles, our results for CH^-; solid green stars, our results for C_2H^-; open inverted triangles, F^- [47]; open stars, Cl^- [47]; crosses, Br^- [47]; open rhombi, I^- [47]; half-filled circles, Ref. [40]; open upward triangles, Cl^- [48]; open circles, Br^- [48]; open squares, I^- [48]; solid line, H^- [38], dotted line, $e^- + N_2$ [46].

associated with the electron-impact excitation of N_2 in the Π_u state are responsible for a large peak around the electron velocity of approximately 0.4 a.u. [46]. In fact, we note from Fig. 8 that all cross sections shown present a peak-shaped structure around 0.4 a.u. This explains the monotonically decreasing (increasing) behavior for the cross sections of C^- (C_2^-) in the velocity range shown here. By using a simple theoretical model, where the outermost electron velocity distribution was convoluted with the total electron-scattering cross sections, Jalbert *et al.* [45] were able to reproduce this effect, which was suggested to be universal for each target system, i.e., independent of the anion type. In this scenario, the differences between cross sections of different anions impacting on N_2 are, in a first approximation, correlated to the anion size, as described in the geometrical picture of Ref. [47].

In Fig. 8, the C_n^- ($n = 1,2$) cross sections are compared with the TED cross sections of the first four halogen anions, for these anions have comparable ionic radii to that of C^-. A compilation of TED cross-section data for the hydrogen anion is also displayed in Fig. 8. As we note from Fig. 8, our cross-section values for C^- lie between the F^- and I^- values, which is consistent with the geometrical picture, given that the former corresponds to the smallest ionic radius while the latter has the highest radius between the atomic anions showed here. In Fig. 8, we also display the result obtained by the group of Ishikawa *et al.* [40] for C^-. We note that their cross-section value is above all the other cross sections displayed in Fig. 8. All the other cross sections for the destruction of C^- presented in Fig. 7 lie below the value of the F^- cross section; therefore, we believe that our values for the total collisional destruction cross sections of C^- on N_2 are the most accurate ones.

IV. SUMMARY AND CONCLUSIONS

We produce C_n^- and C_nH^- ($n = 1,2$) anions by sputtering of cesium on a carbon-rich sample containing hydrogen peroxide. In order to measure their total electron detachment cross section as a function of the anion's velocity, the C_n^- and C_nH^- ($n = 1,2$) anions' attenuation currents are measured after they traverse a gas chamber containing molecular nitrogen as a function of gas pressure. The analysis of the attenuation curves also shows that there is no sign of an undesirable metastable components of the C^- beam used.

TABLE I. TED cross-section values (10^{-15} cm^2). The uncertainties are 12%.

Energy (keV)	C^-	CH^-	C_2^-	C_2H^-
30		2.22	2.09	2.18
35	2.01	1.99	2.15	2.36
40	1.99	2.03	2.59	2.14
45	1.98		2.14	
50	2.05	2.21		2.52
55	1.99			2.51
60			2.67	2.61
65	2.01	2.02		2.38
70			2.78	
75	1.87	2.07		
80			2.62	2.74
85	1.80	2.05		
90				2.63
95	1.82	2.07		
100			2.64	

Our cross section values for the collisional destruction of C^- on N_2 are compared with those of other groups, and strong discrepancies have been found. In order to access the problem, we compared our results to the collisional destruction data of other anions measured by three different groups. This comparison shows that our results are consistent with the geometrical picture described by Sant'Anna *et al.* [47] and results for hydrogen and halogen projectiles measured by different experimental groups [38,48]. The present work provides the values (see Table I) for the total electron detachment cross sections of C_n^- and C_nH^- ($n = 1,2$) colliding with N_2 in the velocity range of 0.22 to 0.56 a.u.

Together with experimental data for other anionic projectiles, our data point to a universal behavior of cross sections related to a shape resonance present in total electron scattering by N_2. This suggests a criterion for choosing important electronic states to be taken into account in future theoretical calculations for collision systems involving CH^- and C_2H^- projectiles.

ACKNOWLEDGMENTS

This work was partially supported by the Brazilian agencies CNPq, CAPES, FAPERJ, and FUJB and by the Rede Nacional de Fusão–Brasil.

[1] L. H. Andersen, C. Brink, H. K. Haugen, P. Hvelplund, and D. H. Yu, Chem. Phys. Lett. **217**, 204 (1994).
[2] M. L. Gardela, R. Vandenboschb, B. P. Henry, C. Cooperc, and D. I. Will, Eur. Phys. J. D **7**, 79 (1999).
[3] T. Pino, M. Tulej, F. Güthe, M. Pachkov, and J. P. Maier, J. Chem. Phys. **116**, 6126 (2002).
[4] V. Wakelam *et al.*, Astrophys. J. Suppl. Ser. **199**, 21 (2012).
[5] G. Halmová and J. Tennyson, Phys. Rev. Lett. **100**, 213202 (2008).
[6] A. Faure, V. Vuitton, R. Thissen, and L. Wiesenfeld, J. Phys. Chem. **113**, 13694 (2009).
[7] T. R. Taylor, C. Xu, and D. M. Neumark, J. Chem. Phys. **108**, 10018 (1998).
[8] P. Chaizy, H. Rème, J. A. Sauvaud, C. d'Uston, R. P. Lin, D. E. Larson, D. L. Mitchell, K. A. Anderson, C. W. Carlson, A. Korth, and D. A. Mendis, Nature (London) **349**, 393 (1991).
[9] A. J. Coates, A. Wellbrock, G. R. Lewis, G. H. Jones, D. T. Young, F. J. Crary, and J. H. Waite, Jr., Planet. Space Sci. **57**, 1866 (2009).
[10] A. J. Coates, G. H. Jones, G. R. Lewis, A. Wellbrock, D. T. Young, F. J. Crary, R. E. Johnson, T. A. Cassidy, and T. W. Hill, Icarus **206**, 618 (2010).

[11] D. J. Goebbert, D. Khuseynov, and A. Sanov, J. Chem. Phys. **131**, 161102 (2009).
[12] J. Cernicharo, M. Guélin, M. Agúndez, K. Kawaguchi, M. McCarthy, and P. Thaddeus, Astron. Astrophys. **467**, L37 (2007).
[13] M. C. McCarthy, C. A. Gottlieb, H. Gupta, and P. Thaddeus, Astrophys. J. **652**, L141 (2006).
[14] S. Brünken, H. Gupta, C. A. Gottlieb, M. C. McCarthy, and P. Thaddeus, Astrophys. J. **664**, L43 (2007).
[15] M. Agúndez *et al.*, Astron. Astrophys. **517**, L2 (2010).
[16] P. Thaddeus, C. A. Gottlieb1, H. Gupta, S. Brünken, M. C. McCarthy, M. Agúndez, M. Guélin, and J. Cernicharo, Astrophys. J. **677**, 1132 (2008).
[17] J. Cernicharo, M. Guélin, M. Agúndez, M. C. McCarthy, and P. Thaddeus, Astrophys. J. **688**, L83 (2008).
[18] O. May, J. Fedor, B. C. Ibănescu, and M. Allan, Phys. Rev. A **77**, 040701(R) (2008).
[19] A. J. Coates F. J. Crary, G. R. Lewis, D. T. Young, J. H. Waite Jr., and E. C. Sittler Jr., Geophys. Res. Lett. **34**, L22103 (2007).
[20] J. Winter, Plasma Phys. Controlled Fusion **40**, 1201 (1998).
[21] J. Winter, Plasma Phys. Controlled Fusion **46**, B583 (2004).
[22] V. Vuitton, P. Lavvas, R. V. Yelle, M. Galand, A. Wellbrock, G. R. Lewis, A. J. Coates, and J.-E. Wahlund, Planet. Space Sci. **57**, 1558 (2009).
[23] R. D. Thomas *et al.*, Rev. Sci. Instrum. **82**, 065112 (2011).
[24] K. Abrahamsson *et al.*, Nucl. Instrum. Methods Phys. Res., Sect. B **79**, 269 (1983).
[25] J. W. Xia *et al.*, Nucl. Instrum. Methods Phys. Res., Sect. A **488**, 11 (2002).
[26] D. Krämer *et al.*, Nucl. Instrum. Methods Phys. Res., Sect. A **287**, 268 (1990).
[27] T. Tanabe, K. Nodaa, T. Honmab, M. Kodairac, K. Chida, T. Watanabe, A. Nodad, S. Watanabe, A. Mizobuchi, M. Yoshizawa, T. Katayama, and H. Muto, Nucl. Instrum. Methods Phys. Res., Sect. A **307**, 7 (1991).
[28] A. Naaman, K. G. Bhushan, H. B. Pedersen, N. Altstein, O. Heber, M. L. Rappaport, R. Moalem, and D. Zajfman, J. Phys. Chem. **113**, 4662 (2000).
[29] A. M. Covington *et al.*, Phys. Rev. A **66**, 062710 (2002).
[30] R. Middleton and C. T. Adams, Nucl. Instrum. Methods **118**, 329 (1974).
[31] H. Luna, F. Zappa, M. H. P. Martins, S. D. Magalhães, G. Jalbert, L. F. S. Coelho, and N. V. de Castro Faria, Phys. Rev. A **63**, 052716 (2001).
[32] H. Luna, S. D. Magalhães, J. C. Acquadro, M. H. P. Martins, W. M. S. Santos, G. Jalbert, L. F. S. Coelho, and N. V. de Castro Faria, Phys. Rev. A **63**, 022705 (2001).
[33] F. Zappa, L. F. S. Coelho, S. D. Magalhães, J. C. Acquadro, T. S. Cabral, G. Jalbert, and N. V. de Castro Faria, Phys. Rev. A **64**, 032701 (2001).
[34] F. Zappa, L. F. S. Coelho, S. D. Magalhães, W. M. S. Santos, A. M. Luiz, M. H. P. Martins, A. L. F. de Barros, J. A. M. Pereira, and N. V. de Castro Faria, Phys. Rev. A **67**, 012702 (2003).
[35] M. M. Sant'Anna, F. Zappa, A. C. F. Santos, L. F. S. Coelho, W. Wolff, A. L. F. de Barros, and N. V. de Castro Faria, Phys. Rev. A **74**, 022701 (2006).
[36] G. Jalbert, L. Silva, W. Wolff, S. D. Magalhães, A. Medina, M. M. Sant'Anna, and N. V. de Castro Faria, Phys. Rev. A **74**, 042703 (2006).
[37] N. V. de Castro Faria, M. M. Sant'Anna, C. Carvalho, G. Jalbert, L. F. S. Coelho, B. Magnani, and F. Zappa, Int. J. Quantum Chem. **111**, 1836 (2012).
[38] Y. Nakai, T. Shirai, T. Tabata, and R. Ito, At. Data Nucl. Data Tables **37**, 69 (1987).
[39] A. Aguilar, A. M. Covington, G. Hinojosa, R. A. Phaneuf, I. Álvarez, C. Cisneros, J. D. Bozek, I. Dominguez, M. M. Sant'Anna, A. S. Schlachter, S. N. Nahar, and B. M. McLaughlin, Astrophys. J. Suppl. Ser. **146**, 467 (2003).
[40] J. Ishikawa, H. Tsuji, and T. Takagi, Vacuum **36**, 887 (1986).
[41] M. Matić and B. Čobić, J. Phys. B **4**, 111 (1971).
[42] I. S. Dimitriev, V. S. Nikolaev, Ya. A. Teplova, B. M. Popov, and L. I. Vinogradova, Zh. Eksp. Teor. Fiz. [Sov. Phys. JETP] **23**, 832 (1966).
[43] I. T. Serenkov, R. L. Ilin, and V. A. Oparin, Zh. Tekh. Fiz. [Sov. Phys. Tech. Phys.] **22**, 515 (1977).
[44] I. T. Serenkov, R. L. Ilin, V. A. Oparin, and E. S. Solov'ev, Sov. Phys.-JETP **41**, 845 (1975).
[45] G. Jalbert, W. Wolff, S. D. Magalhães, and N. V. de Castro Faria, Phys. Rev. A **77**, 012722 (2008).
[46] Y. Itikawa, J. Phys. Chem. Ref. Data **35**, 31 (2006).
[47] M. M. Sant'Anna, F. Zappa, A. C. F. Santos, A. L. F. de Barros, W. Wolff, L. F. S. Coelho, and N. V. de Castro Faria, Plasma Phys. Controlled Fusion **46**, 1009 (2004).
[48] W. J. Lichtemberg, K. Bethge, and H. Schmidt-Bocking, J. Phys. B **13**, 343 (1980).